

HIGH SPEED LASER STRUCTURING OF CRYSTALLINE SILICON SOLAR CELLS

S. Eidelloth, T. Neubert, T. Brendemühl, S. Hermann, P. Giesel, and R. Brendel
Institut für Solarenergieforschung Hameln (ISFH), Am Ohrberg 1, D-31860 Emmerthal, Germany

ABSTRACT

Fast laser processing is commonly done using laser beams with Gaussian beam profiles in combination with scanning optics. Single laser pulses only affect a limited area beneath the Gaussian intensity bell and result in circular impact regions. Adjacent impact regions have to overlap considerably when continuous processing larger areas. Thus, the processing speed is greatly enhanced by replacing the Gaussian profile with a flat-top intensity profile and by replacing the radial symmetric cross section with a rectangular beam cross section. However, processing with a rectangular flat-top laser beam through a scanner has, to the best of our knowledge, not yet been demonstrated. We report on the successful design and experimental tests of a new laser system that images a rectangular flat-top laser beam through a scanner. Our so-called Simultaneous Scanning and Laser Beam Imaging – system (SIMSALABIM) machines a finger pattern that covers 50 % of a (125 x 125) mm² crystalline Si solar cell in 14 s. Two parallel slab lasers with increased output power should process the same area in just 2.5 s.

INTRODUCTION

High efficiency, wafer based cell concepts call for well defined geometric patterns. Photolithography is expensive. Therefore alternative processes like inkjet printing or laser structuring need to be pushed to a level capable of meeting industrial needs. Laser machining tends to result in higher investment, but lower cost of operation compared to printing. How to further reduce laser process times and therefore increase wafer throughput is the topic of this paper. We compare the structuring index (distance between the centres of two single impact regions) of round Gaussian beams and rectangular flat-top beams. We also discuss structuring times for finger shaped geometries.

The geometry after the scanning mirrors would lie on a curved plane without a so called f-theta lens. We need the f-theta lens to homogeneously machine the flat wafers. When a Gaussian laser beam propagates through an f-theta lens it approximately stays Gaussian, because the Fourier transform of a Gaussian profile again is a Gaussian profile. Thus, the f-theta lens of the scanner has no crucial impact on the Gaussian intensity profile of the laser beam.

However, a rectangular flat-top intensity profile is not invariant to Fourier transformation. We describe a new laser system that Fourier transforms the shaped laser beam before the scanner. The f-theta lens then performs a reverse transformation. Thus, we get the wanted intensity

profile at the wafer surface. Our SIMSALABIM system paves the way for joining high speed scanning with the benefits of beam shaping.

STRUCTURING INDEX AND SINGLE PULSE ABLATION AREA

Laser structuring, like edge isolation, is commonly performed by a beam with Gaussian-like intensity profile

$$I(x, y, z) \approx I_0(z) e^{-\frac{x^2 + y^2}{w(z)^2}}, \quad (1)$$

with

$$I_0(z) = \frac{W_0}{w(z)} I_{\max} \quad (2)$$

and

$$\frac{w(z)^2}{w_0^2} - \frac{z^2}{Z_R^2} = 1. \quad (3)$$

The ablation area $A(z)$ in a simplistic model (see Fig. 1) only depends on the ablation threshold intensity I_{th} , the maximum intensity $I_0(z)$, and the beam radius $w(z)$.

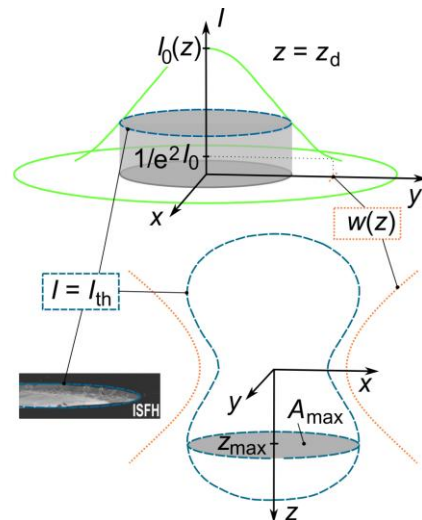


Fig. 1: Schematic intensity distribution of a Gaussian laser beam. - Threshold intensity I_{th} , maximum intensity $I_0(z)$ and beam radius $w(z)$ define the ablation area A at a definite position z_d in propagation direction z . The maximum ablation area A_{max} results at the optimum position z_{max} .

If the beam geometry is fixed (installed optics define the Rayleigh length z_R of the Gaussian beam and therefore the hyperbolic shape in propagation direction z is fixed), the maximum ablation area A_{max} is obtained (see Fig. 1) at a corresponding position

$$z_{max} = \begin{cases} \pm z_R \sqrt{\frac{I_{max}}{e I_{th}} - 1} & I_{max} > e I_{th} \\ 0 & I_{max} \leq e I_{th} \end{cases} \quad (4)$$

This optimum position generally depends on the maximum Intensity I_{max} in the beam, the Rayleigh length z_R and the ablation threshold intensity I_{th} of the material.

The maximum size A_{max} of the round ablation area as function of laser pulse energy E_p and pulse duration t_p can be estimated for ideal beam geometry with

$$A_{max} = \frac{1}{e} \frac{E_p}{t_p I_{th}} \quad (5)$$

For ablating a continuous line, the round spots are projected with the spot overlap δ_{circle} onto the wafer surface. The according structuring Index d_{gauss} (that is the distance between the centers of two adjacent single pulse impact regions) becomes [1] :

$$d_{gauss} = (1 - \delta_{circle}) \sqrt{\frac{4}{e \pi} \frac{E_p}{t_p I_{th}}} \quad (6)$$

The “volume” beneath the Gaussian bell in Fig. 1 corresponds to the power P of the laser pulse. The cap and the surrounding part of the bell are lost, because only the inner “power-cylinder” is utilized for the ablation process. Therefore, structuring with a flat-top cuboid at same pulse energy and square beam cross section results in a larger structuring index $d_{flat-top}$:

$$d_{flat-top} = (1 - \delta_{square}) \sqrt{\frac{E_p}{t_p I_{th}}} \quad (7)$$

Rectangles need less spot overlap than circles and with spot overlaps $\delta_{circle} \approx 0.3$ and $\delta_{square} \approx 0.15$ a theoretical time yield factor of $d_{flat-top}/d_{gauss} = 1.8$ for line ablation is achieved, comparing round Gaussian profiles and flat-top profiles with a square cross section. Possible disadvantages of shaped beams are power losses through the beam shaping optics, shorter depth of focus and lower pattern resolution.

PROCESS TIME

We primarily concern two components of the total process time:

t_s : Pure structuring time, depending on geometry of pattern, structuring indices (d_x , d_y), laser pulse repetition rate f_R and scanning velocity v_s respectively.

t_r : Ramping & return time for scanning mirror acceleration/deceleration, depending on the number of structuring lines N , scanning velocity v_s , mirror weight, etc.

The laser machining of a wafer in practice starts with wafer handling and image recognition. Additionally, the total process time includes idle jumping time for the mirrors to jump between separate parts of the scanned geometry (this is negligible in our case).

Pure structuring time

There are two limiting scenarios for the pure structuring time. In the first scenario the minimum time is limited by the velocity of the scanning mirrors (scanner limited). In the second scenario it is limited by the size of the structuring index in combination with the laser pulse repetition rate f_R (laser limited). We discuss both scenarios in detail and consider a finger pattern which is shown in Fig. 2.

This pattern includes a busbar for a full-squared wafer. The preferred scanning direction for the busbar is perpendicular to the direction for finger scanning. In Fig. 3 the whole pattern is scanned in one direction. This structuring mode is favored for more complex pseudo-square patterns (depending on scanning parameters, pattern geometry and spot size).

We use the overlap factor δ to generally compare the structuring indices for circular and square shaped single pulse impact regions above. The following discussion specifically applies to rectangular ablation areas $A = b h$ (we have a rectangular flat-top intensity profile) and assumes a constant overlapping distance d_o .

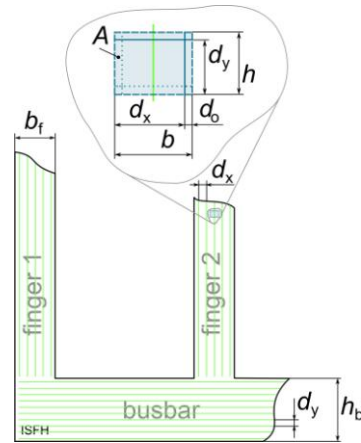


Fig. 2: Finger geometry with busbar. - In practice, it is not possible to utilize the entire ablation area $A = b h$ of a single laser pulse. The areas need to overlap by a distance d_o in order to reliably achieve a complete coverage. A scanning process fills the finger geometry with lines, having a distance d_x to each other and an internal structuring index d_y . Line distance and structuring index are interchanged for busbar scanning in perpendicular direction to that of the fingers.

The line internal structuring index thus becomes $d_x = b - d_o$ for busbar scanning and $d_y = h - d_o$ for finger scanning in the perpendicular direction. We calculate the corresponding scanning velocity

$$v_{s,y} = f_R d_y \quad (8)$$

in finger direction for a given laser pulse repetition rate f_R .

When optimizing f_R , one has to keep in mind, that the line index d_x and the number of lines per finger n_f have to fit the finger width b_f , using a small overlap d_o and following the equation

$$n_f d_x = b_f - d_o. \quad (9)$$

The pure structuring time

$$t_{sf} = N \frac{h_f}{v_{s,y}} = N_f \frac{b_f - d_o}{d_x} \frac{h_f}{f_R d_y} \quad (10)$$

applies for the total N lines of the N_f fingers (width b_f , length h_f , without busbar height h_b). Assuming the single pulse ablated area A to be constant for different aspect ratios, the time

$$t_{sf} = N_f \frac{b_f - d_o}{d_x} \frac{h_f}{f_R \left(\frac{A}{d_x + d_o} - d_o \right)} \quad (11)$$

is written as a function of the line index d_x . It has a minimum

$$t_{sf,\square}(f_R) = \frac{N_f h_f}{f_R} \frac{b_f - d_o}{\sqrt{A(f_R)} - d_o} \quad (12)$$

for an optimum index

$$d_x = d_y = \sqrt{A} - d_o \quad (13)$$

and a corresponding optimum velocity

$$v_{s,\text{opt}} = f_R (\sqrt{A} - d_o). \quad (14)$$

Thus, the aspect ratio should be 1 (the cross section of the laser spot should be a square).

Furthermore, the minimum structuring time $t_{sf,\text{min}}$ is reached at an optimum laser repetition rate $f_{R,\text{opt}}$, depending on the function $A(f_R)$. This function is characteristic for a specific machining process and laser system. The area A generally depends on $E_p(f_R)$, $t_p(f_R)$ and $I_{th}(t_p)$. The pulse energy E_p stored in the active media of a laser usually decreases with increasing f_R . It sometimes can be described like an "unloading curve of a capacitor":

$$E_p(f_R) = E_{\text{max}} \left(1 - e^{-\frac{1}{\tau f_R}} \right) \quad (15)$$

However, the real output of lasers might definitely deviate from this behavior. Pulse duration $t_p(f_R)$ and threshold intensity $I_{th}(t_p)$ are taken constant in this approach. We assume A to be approximately proportional to the pulse energy $E_p(f_R)$. Thus, the ablation area $A(f_R)$ usually decreases with increasing laser pulse repetition rate f_R .

In our first scenario the optimum ablation velocity $v_{s,\text{opt}}$ is too high for the scanner. It is not possible to get discrete spots onto the wafer and the process is scanner limited. We assume a scanning velocity limit of 15 m/s. For a laser system with a high repetition rate of $f_R = 1$ MHz an ablation area larger than $(15 \times 15) \mu\text{m}^2$ is required to reach this limit. The next generation of picosecond lasers (or even some currently available lasers, see e.g. [2]) should be able to achieve this specification. With small ablation areas A the number of lines N and therefore the ramping and return time t_r (see below) would be large, even rising the demand in scanning speed. If one chooses such a scanner limited process it might be advantageous to reduce the line number N by shaping the beam rectangular (short side of rectangle would parallel the scanning direction).

We put the second scenario into practice for our SIMSALABIM system. Our process is laser limited and works with large single pulse ablation areas at a low laser pulse repetition rate of 50 kHz. Even with next generation slab lasers this kind of process is likely to stay laser limited for the near future. If we consider for example a structuring index of $d_x = d_y = 150 \mu\text{m}$ the laser system would have to deliver a laser pulse repetition rate of $f_R = 100$ kHz to reach the scanner limit. A lot of pulse energy has to be stored in the laser active media to ablate an area larger than $(150 \times 150) \mu\text{m}^2$. Furthermore the laser wavelength and the pulse duration have to be low, granting low laser induced silicon damage [3]. These specifications are hard to achieve.

Ramping & return time

Our machining programs include acceleration and deceleration ramps for each line to ensure constant structuring index d_y . Within a single ramping & return time t_{r1} the scanning mirrors deflect the laser beam to the next line's starting point and velocity (see Fig. 3).

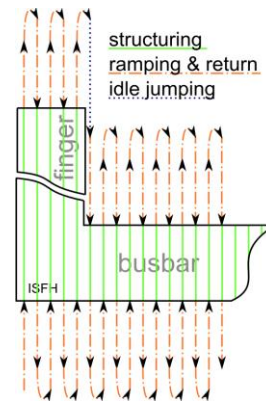


Fig. 3: Scanning path, including structuring path, ramping & return path and idle jumping path.

With constant angular acceleration of the mirrors the ramping & return times are a function of the scanning velocity. Then for short (busbar) lines, it could be helpful to reduce structuring velocity. The structuring time would increase, but ramping & return time would decrease, decreasing total process time.

However, our scanner controller does not use a constant acceleration. The controller automatically adjusts the acceleration as function of scanning velocity: for low line structuring speed low ramp accelerations apply. The acceleration time of our scanner (hurrySCANII 14, SCANLAB AG) is 0.3...0.4 ms for angular speeds ≤ 50 rad/s and the acceleration is not constant within the acceleration time. Our single ramping & return time t_{r1} stays constant at about 1 ms, independent of structuring speed. Therefore, with our current scanner controller we are not able to optimize the scanner acceleration and speed as function of the line length.

Let us now estimate the process time for industrial machining with a next generation slab laser ($P_{av} \approx 200$ W) of a (125 x 125) mm² pseudo square wafer. A laser limited process, scanning 256 finger lines with a length of $h_f = 125$ mm at $v_s = 10$ m/s theoretically takes $t_s = 2.3$ s pure structuring time. Adding another 253 busbar lines with an average length of $h_b = 3$ mm results in a total pure structuring time of $t_s = 2.38$ s. Ramping & return with $t_{r1} = 1$ ms and 509 lines would finally increase the process time to $t = 2.9$ s. Thus, with two parallel slab lasers the process time should be below 2.5 s, including wafer handling, image recognition and idle jumping.

For the scanner limited scenario with high repetition rate lasers and low line distances the ramping & return time gets more important. As an example we increase the line number by a factor of 10 to increase the pattern resolution. Then the scanning velocity v_s would have to be increased and the single ramping & return time t_{r1} would have to be decreased by the same factor to keep the process time constant. This high line number kind of process could be realized with the application of high repetition rate lasers and polygon scanners. Polygon scanners should allow for scanning speeds > 50 m/s and the return time would correspond to the small gate time for blending out mirror edges. However, polygon scanners are not commercially available for our applications yet.

SIMSALABIM SYSTEM

Figure 4 shows the components of our home-built Simultaneous Scanning and Laser Beam Imaging - system (SIMSALABIM).

One of the advantages of our INNOSLAB laser ($\lambda = 532$ nm, $t_p \approx 10$ ns, $P_{av} \approx 50$ W @ $f_R = 50$ kHz, Edgewave GmbH) is its resonator shape. The output beam already has a flat-top intensity distribution in unstable resonator direction [4]. The Gaussian shape in stable resonator direction is transformed to a flat-top intensity shape by means of a beam shaping module, directly attached to the slab laser. Lenses (l_1, l_2, l_3) and mirrors (m_1, m_2) guide the shaped laser beam to the scanner.

The schematic of our optical assembly is shown in Fig. 5a. A telescope (consisting of the f-theta lens l_4 and

two additional lenses l_2, l_3) images the intensity profile down to the substrate. The task of the first lens l_1 is to supply the telescope with the already shaped laser beam at required object position. This optical setup was proposed by Edgewave GmbH. We use an f-theta lens with a focal length large enough ($f = 0.25$ m) to machine (156 x 156) mm² wafers. This results in a total optical path length of approximately 1.5 m.

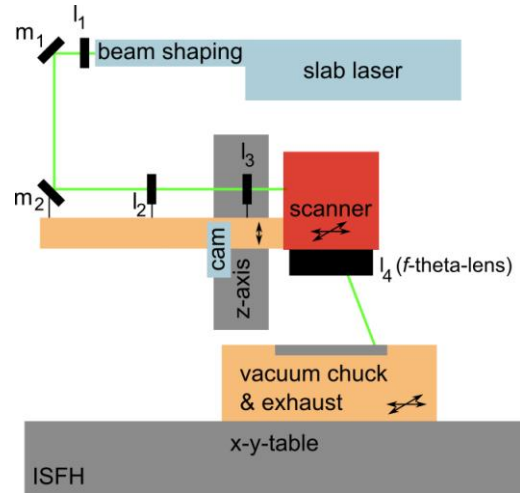


Fig. 4: Components of our home build SIMSALABIM system.

Figure 5b shows the principle of our SIMSALABIM system. The left telescope lens represents the optics l_2, l_3 and results in a Fourier transformation of the squared flat-top profile. The right telescope lens of the principle figure represents the f-theta lens of the scanner and thus the reverse transformation. Behind the telescope an image of the object is projected onto the wafer surface and results in square like ablation areas (see Fig 9).

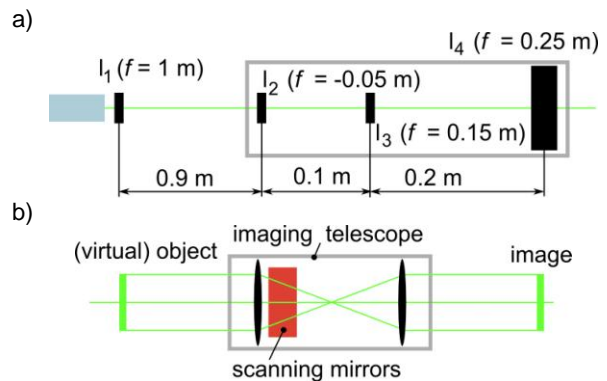


Fig. 5: Optical assembly a) and principle b) of the SIMSALABIM system.

We place scanning mirrors inside the telescope to move the image and structure the geometry pattern. (Since the intensity inside the telescope is concentrated one has to keep in mind not to exceed the damage threshold of the scanning mirrors.) Thus our process

simultaneously deflects and images the laser beam. To the best of our knowledge this is the first time a flat-top intensity distribution was guided through a scanner for high speed laser structuring of solar cells. Our SIMSALABIM system thus paves the way for joining high speed scanning with the benefits of beam shaping.

EXPERIMENTAL ESTIMATION OF OPTIMUM LASER REPETITION RATE

We measure the average output power $P_{av}(f_R)$ of our SIMSALABIM system after the scanner and determine the pulse energy $E_p = P_{av} / f_R$ (Fig. 6a). The average output power and pulse energy of our picosecond laser system (utilizing a SUPER RAPID laser from LUMERA LASER GmbH) is shown in Fig. 6b for comparison.

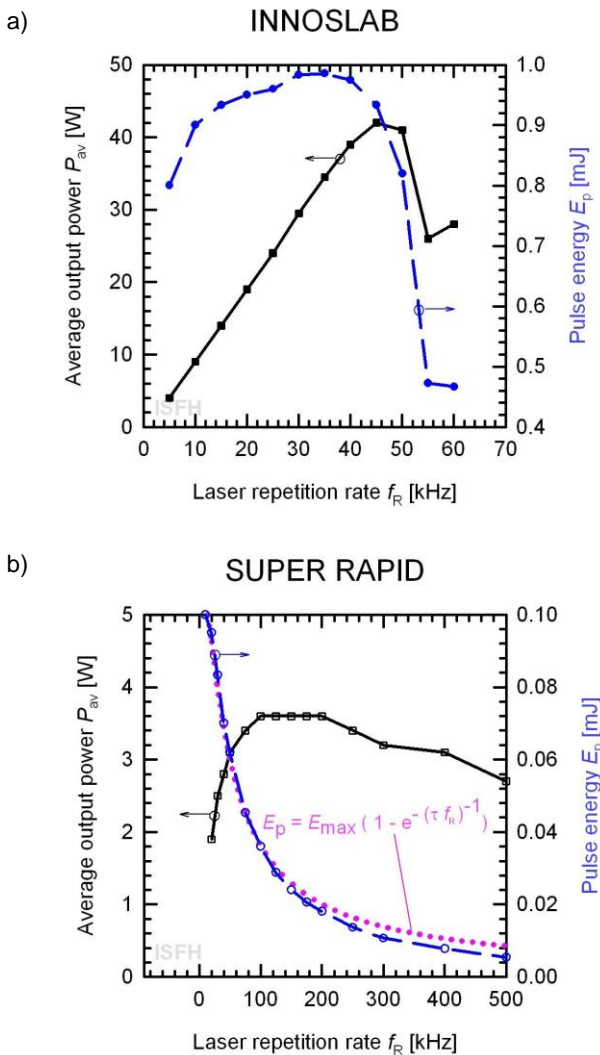


Fig. 6: Average output power P_{av} and pulse energy E_p . - a) Our SIMSALABIM system includes an INNOSLAB laser. b) The output of another laser system with a SUPER RAPID picosecond laser is shown for comparison. Its pulse energy behaves like an “unloading curve”.

The pulse energy in Fig. 6b is fitted with a dotted line and approximately behaves like an “unloading curve” (15). The pulse energy E_p of the SIMSALABIM system first increases with increasing laser repetition rate f_R and then decreases. The optimum repetition rate $f_{R,opt}$ is not obvious at a first glance. We assume the pulse energy E_p to be proportional to the single pulse ablation area A . Using this approximation and neglecting the influence of d_b we can simplify equation (12). The pure structuring time $t_{str}(f_R)$ is approximately inversely proportional to the product

$$\rho_v = f_R \sqrt{E_p(f_R)} \quad (16)$$

of repetition rate and square root of pulse energy.

This characteristic product ρ_v is shown in Fig. 7. The product ρ_v of our SIMSALABIM slab laser system (INNOSLAB) has its optimum laser repetition rate at $f_{R,opt} = 50$ kHz. The maximum of the characteristic product of our slab laser system is larger than that of our picosecond laser system.

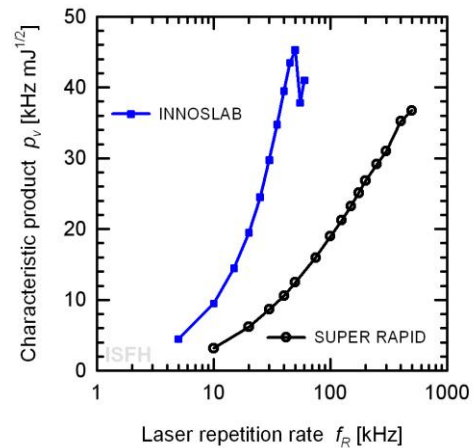


Fig. 7: Characteristic product ρ_v for our SIMSALABIM slab laser system (INNOSLAB) and our picosecond laser system (SUPER RAPID). - The maximum of the product ρ_v (laser repetition rate times square root of pulse energy) results in minimum process time, if the pulse energy is proportional to the single pulse ablation area and the machining process is not scanner limited.

RAMP LENGTH

The lengths of acceleration and deceleration ramps of our SIMSALABIM slab laser system are shown in Fig. 8. We use 1.52 mm ramp length for acceleration and 1.25 mm for deceleration at a scanning velocity of $v_s = 7$ m/s. The reason for different ramp lengths for acceleration and deceleration is not yet clarified, but may originate from the scanner controller or a difference in the “laser on” and “laser off” delay. The ramps are required to grand constant spot distances at the start and at the end of the structuring lines. The ramp lengths increase with increasing structuring velocity. As explained above, the time for ramping & return stays constant at $t_1 \approx 1$ ms.

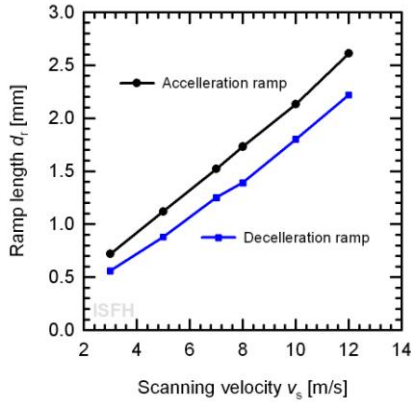


Fig. 8: Length of acceleration and deceleration ramps d_r as function of scanning velocity v_s .

EXPERIMENTAL PROCESS TIME

We machine oxidized Si wafers using the above described SIMSALABIM system at the optimum laser repetition rate $f_{R,opt} = 50$ kHz. Figure 9 shows single pulse ablation areas. The approximately squared patterns do not show any remaining silicon oxide islands inside the opened areas.

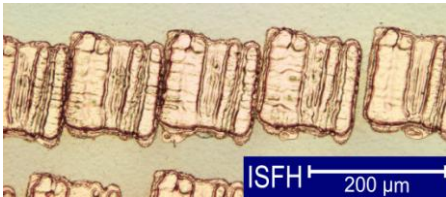


Fig. 9: Optical microscope image of slab laser ablation areas on an oxidized silicon wafer.

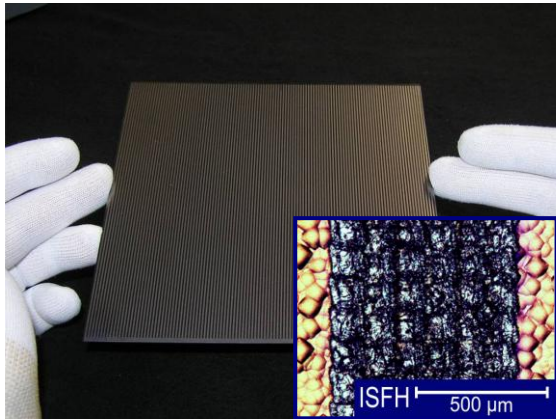


Fig. 10: Photograph and optical microscope image of a finger pattern. - Machined with a quasi square flat-top intensity profile through a scanner on an oxidized silicon wafer.

In order to structure a geometric pattern we ablate overlapping lines with a speed of $v_{s,opt} = 7$ m/s. The photograph of such a pattern on a full-squared wafer is shown in Fig. 10. We also machine more complex patterns on pseudo-square wafers. A finger pattern (including busbar) that covers 50 % of a (125 x 125) mm² pseudo-square wafer takes 14 s (without handling and image recognition).

CONCLUSIONS & OUTLOOK

Simultaneous Scanning and Laser Beam Imaging (SIMSALABIM) allows for high-speed laser machining with rectangular flat-top intensity profiles. Our SIMSALABIM process is not limited to wafer substrates and could be applied to all processes calling for a special intensity profile. Edge isolation, marking, cutting and laser doping are a few examples. Machining with a squared flat-top intensity profile instead of a round Gaussian profile theoretically increases the line processing velocity by a factor of 1.8.

There are two possibilities how to significantly reduce our current process time of 14 s. One is to use a (currently available) high repetition rate laser system ($f_R > 1$ MHz). Polygon scanners would have to be developed for this application because they can offer the required high scanning velocities and low return times.

Our current structuring process time of 14 s with a single slab laser system is limited by the output power and repetition rate ($P_{av} \approx 50$ W, $f_R = 50$ kHz) of our slab laser. With 2 parallel SIMSALABIM systems and next generation slab lasers ($P_{av} \approx 200$ W) industrial wafer structuring will be possible within 2.5 s.

ACKNOWLEDGEMENTS

The authors would like to thank Dr. Du, Edgeway GmbH, for custom product development and help with optical design. We also thank Dr. Harder, ISFH for fruitful discussions. The financial support by the German ministry of BMU for the project LaserInvest (No. 0327547A) is gratefully acknowledged.

REFERENCES

- [1] P. Engelhart, *Lasermaterialbearbeitung als Schlüsseltechnologie zum Herstellen rückseitenkontaktierter Siliciumsolarzellen*, PhD thesis, 2007, pp. 87-88, Leibnitz University Hannover.
- [2] Data sheet of HYPER RAPID 50, LUMERA LASER GmbH, 2009
- [3] S. Eidelloth, *Untersuchung von laserinduzierten Schädigungen bei der Strukturierung von Siliziumwafern für Hocheffizienz-Solarzellen*, Diploma thesis, 2006, University of Applied Sciences Münster
- [4] Product information sheets of Edgeway GmbH, 2009.